

Image Sharpening with Waveform Compensation for the Frequency-Domain DORT with a Single-Antenna UWB Radar

Takuya Sakamoto* and Toru Sato
Graduate School of Informatics, Kyoto University
Yoshida-Honmachi Sakyo-ku, Kyoto 606-8501, Japan
Email: t-sakamo@i.kyoto-u.ac.jp

Abstract—Ultra wide-band (UWB) radar is an attractive technology in a variety of applications including security systems. In that pursuit, it is essential to develop low-cost systems that produces clear target images. We have recently developed an imaging method for a simple radar system with a single antenna, namely the frequency-domain DORT (French acronym for decomposition of the time reversal operator) [1] by extending the conventional DORT [2], [3], [4]. Since a point target is assumed, this method cannot produce clear images for a finite-sized target. As a result, images are blurred and compromise image resolution. This study proposes a radar imaging method that can be applied to a finite-sized target. The method modifies the original frequency-domain DORT by introducing a compensation process for the waveform distortion caused by finite-size effects. The effectiveness of the modified method is established with numerical simulations.

I. INTRODUCTION

Ultra wide-band (UWB) radar is a promising technology that is useful in a variety of applications including surveillance systems. To produce clear images of surveillance targets reliable high-resolution radar imaging systems need to be developed. In search of such systems, Devaney et al. [2] developed the DORT method, which starts by assuming an antenna array and monochromatic sinusoidal signals. It has high-resolution capability by separating multiple propagation paths by applying the singular value decomposition (SVD) to a matrix generated from bi-static measurements with the array antenna [3], [4]. The columns and rows of this matrix correspond to the transmitting and receiving elements, respectively. The matrix for DORT can be generated differently; it can be produced by assigning the column and row to the element number and frequency number respectively, as proposed by Teixeira et al. [5]. Unlike the original DORT, the revised DORT can apply to wideband signals.

These high-resolution DORT methods require antenna array systems that make the system costly and impractical. The need to simplify the system and lower costs is imperative if these methods are to be applied to actual security systems; clearly, the number of antennas must be reduced. Sakamoto and Sato [1] extended the original DORT so that it can be applied to a simple system with a single antenna. Their method, called frequency-domain DORT, generates a matrix to be decomposed by SVD solely in the frequency domain. Numerical simulations and experiments have verified that

the frequency-domain DORT achieves accurate imaging in a multipath environment.

Because the original DORT assumes point-like targets and cannot be applied to finite-sized targets, images obtained using this method are degraded and severely blurred. To tackle this problem, we extend the original frequency-domain DORT by modifying the waveform distorted due to finite-size effects. We measure in advance the scattered waveforms from various sized targets. Scattered signals in a multipath environment are processed using these waveforms with the frequency-domain DORT.

II. SYSTEM MODEL

Figure 1 shows the set-up of the system assumed in this study; a 2-dimensional system comprising a TM (Transverse Magnetic) wave transmitter/receiver is used to estimate the 2-dimensional position of a metallic target. This system is composed of a transmit antenna Tx, a receiving antenna Rx, a plate W made of PEC (Perfect Electric Conductor), and a point-like PEC target P.

The received signals are calculated using FDTD (Finite Difference Time Domain), with 6-layered PML (Perfectly Matched Layer) for absorbing boundaries and a grid size of 1.0 mm. Propagation and scattering field are numerically calculated in the process of imaging in the DORT. The Green's function of a 2-dimensional scalar wave is expressed with a Hankel function of the first kind with argument based on the distance of the propagation path. Scattering by a point target is modeled assuming the Born approximation

$$S(\omega) = \int \omega^2 \sigma(\mathbf{r}') G^2(\omega, \mathbf{r}, \mathbf{r}') d\mathbf{r}', \quad (1)$$

where $\sigma(\mathbf{r}')$ is the relative permittivity at position \mathbf{r}' . The transmitted pulse is a UWB pulse $s_T(t)$, which is assumed to be a mono-cycle pulse. We also assume that the relative locations of antennas and a plate are known. The direct wave $s_D(t)$, propagating without scattering from Tx to Rx, the reflected wave $s_W(t)$ from plate W are measured and stored in memory prior to actual measurements. These waveforms, $s_D(t)$ and $s_W(t)$, are subtracted from the received signal $s_0(t)$ yielding $s(t) = s_0(t) - s_D(t) - s_W(t)$. We assume that $s(t)$ contains four waves, namely

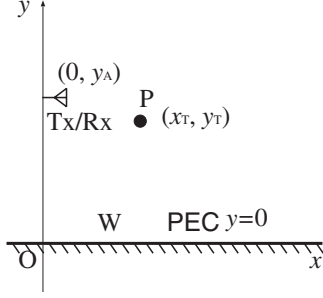


Fig. 1. System model of a multipath scattering UWB radar.

- $s_1(t)$ Tx-P-Rx,
- $s'_2(t)$ Tx-P-W-Rx,
- $s''_2(t)$ Tx-W-P-Rx, and
- $s_3(t)$ Tx-W-P-W-Rx,

where the paths corresponding to $s'_2(t)$ and $s''_2(t)$ are traversed in opposite directions. As a consequence, these echoes cannot be separated if the system satisfies the condition appropriate to the Lorentz reciprocal theorem. Hereafter, by introducing $s_2(t) = s'_2(t) + s''_2(t)$, just three paths are considered. Additionally, note that this model neglects higher-order multiple scattering components.

III. CONVENTIONAL TIME-REVERSAL IMAGING AND DORT

TR imaging, using the Lorentz reciprocal theorem, is distinguished by its simple signal processing. The principle of TR is described below. Let $s(t)$ be the received signal at Rx when a pulse is transmitted from Tx at $t = 0$. Assume that $s(-t)$ is transmitted from Rx, then a strong signal is received at Tx at $t = 0$.

Next, we introduce $G(\omega, \mathbf{r}, \mathbf{r}')$, the Green's function associated with propagation through the medium with inclusion of multipath scattering effects. Using $S_T(\omega)$, the Fourier transform of a transmitted signal $s_T(t)$, then $S(\omega)$, the Fourier transform of the received signal $s(t)$, is expressed as

$$S(\omega) = \omega^2 G^2(\omega, \mathbf{r}, \mathbf{r}') S_T(\omega), \quad (2)$$

disregarding constant terms, and where the positions of both Tx and Rx are taken to be \mathbf{r} while that of the point target is \mathbf{r}' . Here, we have assumed Rayleigh scattering from a tiny scatterer. Note that the time reversal operator is equivalent to complex conjugation. Therefore, the image $I_{\text{TR}}(\mathbf{x})$ from TR method is obtained as

$$\begin{aligned} I_{\text{TR}}(\mathbf{x}) &= \int S^* S_T(\omega) (\omega) G^2(\omega, \mathbf{r}, \mathbf{x}) d\omega, \quad (3) \\ &= \int \omega^2 |S_T(\omega)|^2 G^{*2}(\omega, \mathbf{r}, \mathbf{r}') G^2(\omega, \mathbf{r}, \mathbf{x}) d\omega \end{aligned} \quad (4)$$

$I_{\text{TR}}(\mathbf{x})$ in Eq. (4) takes its maximum value when $\mathbf{x} = \mathbf{r}'$ because the integrand is a real function. As mentioned above, this classical TR method is based on matched filter theory.

DORT is an extension of TR imaging that introduces SVD to improve the resolution. With a space-space matrix K_{SS} , DORT assumes that a sinusoidal wave is transmitted, and there are multiple transmitting and receiving antennas. Element $k_{i,j}$ of K_{SS} is defined as the received complex signal propagating between the i -th transmitting antenna and the j -th receiving antenna. Here, $k_{i,j}$ is expressed as

$$k_{i,j} = \sum_{l=1}^K \sigma_l g_{i,l} g_{l,j}, \quad (5)$$

where $g_{i,l}$ is the Green's function between the i -th antenna and the l -th target, and σ_l is proportional to the scattering intersection of the l -th target. The three terms in Eq. (5) can be divided into three matrices as

$$K_{\text{SS}} = U \Sigma V^H, \quad (6)$$

where U and V are composed of $g_{i,l}$ and $g_{l,j}$, respectively. Here, Σ is a diagonal matrix consisting of diagonal elements σ_l . The Green's function for each propagation path is divided into two matrices U and V , thus enabling an imaging similar to the classical MUSIC method because we can derive a noise subspace by checking the elements of Σ . Although this method works well in the assumed model with a sinusoidal wave and multiple antennas, it cannot be applied to our system with a single antenna. For this reason we need to introduce the frequency-domain DORT discussed in the next section.

IV. FREQUENCY-DOMAIN DORT

S_1, \dots, S_N are defined as the respective values of the received signal $S(\omega)$ in the frequency domain at $\omega_1, \dots, \omega_N$. The matrix K_{FF} is defined as

$$K_{\text{FF}} = \begin{bmatrix} S_1 & S_2 & \cdots & S_L \\ S_{L+1} & S_{L+2} & \cdots & S_{2L} \\ \vdots & \vdots & \vdots & \vdots \\ S_{N-L+1} & S_{N-L+2} & \cdots & S_N \end{bmatrix}, \quad (7)$$

where the rows and columns correspond respectively to coarse and fine changes in frequencies. We assume $N = L^2$ for simplicity. For comparison with the conventional DORT, Fig. 2 shows the SVD of K_{FF} . The Green's function can be approximately decomposed into two parts, a function of a coarse frequency ω and one of a fine frequency $\Delta\omega$. With this approximation, the Green's function for each propagation path can also be divided into two, the associated functions forming the basis of the frequency-domain DORT.

First, the frequency-domain DORT applies SVD to K_{FF} as

$$K_{\text{FF}} = U \Sigma V^H, \quad (8)$$

where Σ is a diagonal matrix with singular values. The left and right singular matrices U and V correspond to coarse and fine frequencies, respectively. As in the conventional DORT, we adopt small $L - PK$ singular values to estimate noise subspaces; where P is the number of multipaths for each point-like target, and K the number of targets. In this paper, we assume $P = 3$ and $K = 1$, choosing left and right singular

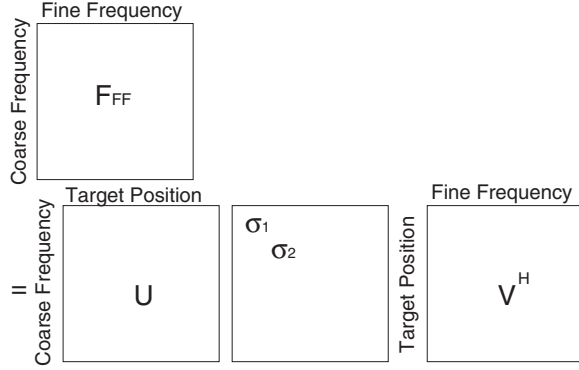


Fig. 2. Singular value decomposition of a space-space matrix in the frequency-domain DORT.

vectors, $\mathbf{u}_{PK+1} \cdots \mathbf{u}_N$ and $\mathbf{v}_{PK+1} \cdots \mathbf{v}_N$, respectively, as base vectors for a noise subspace. The image from the left singular vectors is

$$I_L(\mathbf{x}) = \frac{1}{\sum_{i=PK+1}^L \sum_{p=1}^P |\mathbf{u}_i^H \mathbf{g}_p(\mathbf{x})|^2 / |\mathbf{g}_p(\mathbf{x})|^2}, \quad (9)$$

where \mathbf{g}_p is the L -dimensional vector constructed from values of the Green's function for the p -th path at $\omega_1, \omega_{L+1} \cdots, \omega_{N-L+1}$. The image $I_R(\mathbf{x})$ can be obtained similarly from the right singular vectors. We obtain the final image from their product $I_{DORT}(\mathbf{x}) = I_L(\mathbf{x})I_R(\mathbf{x})$.

V. PROPOSED MODIFIED FREQUENCY-DOMAIN DORT

To apply the frequency-domain DORT to a finite-sized target rather than a point target as assumed above, a modified frequency-domain DORT is presented. The received waveform from a finite-sized target is different from that from a point target.

Figure 3 shows the received signals from cylindrical metallic targets of different radii r ; For each signal three echoes are seen corresponding to the three propagation paths described above. Note that as the radius becomes larger, the echoes are received sooner; creeping echoes are also observed for targets of larger radius.

Figure 4 shows the images calculated using the frequency-domain DORT for these cylindrical targets; images of the larger targets are blurred due to waveform distortion. This is because the frequency-domain DORT employs a vector \mathbf{g}_p that is based on scattering from a single point target. This is of course quite non-physical; the actual situation involves finite-size effects.

Our modified frequency-domain DORT uses the modified Green's function G_m as

$$G_m(\omega, r) = G(\omega)F_0(\omega)/F_r(\omega), \quad (10)$$

$G(\omega)$ is the original Green's function used in the conventional frequency-domain DORT, and $F_r(\omega)$ is the Fourier transform of the waveform scattered from a metallic cylinder with a

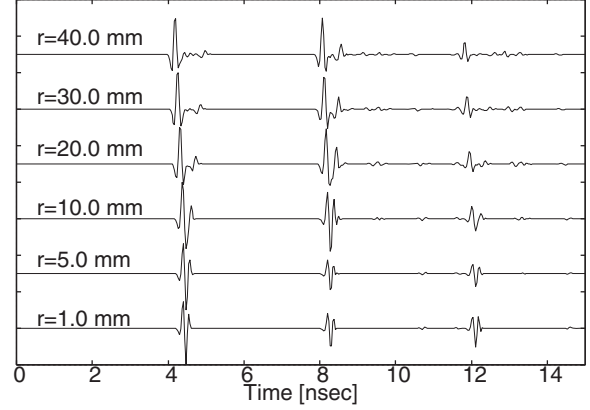


Fig. 3. Received signals from a target with radius r .

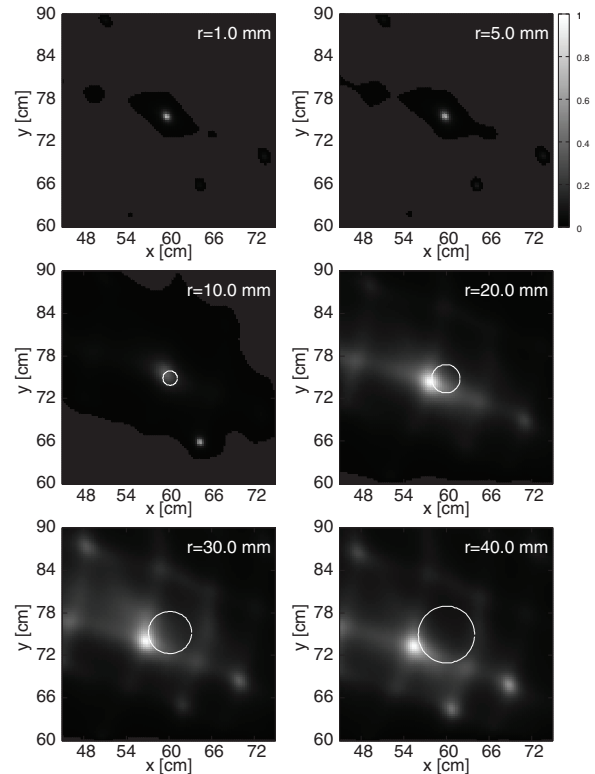


Fig. 4. Images produced by frequency-domain DORT.

radius r . This modified Green's function is used to generate the vector \mathbf{g}_p in Eq. (9) and subsequently to obtain sharper images.

VI. APPLICATION OF PROPOSED METHOD

The left-hand and right-hand side images in Figs. 5, 6 and 7 are respective images produced using the original frequency-domain DORT and the modified frequency-domain DORT, for target radii of 30.0 mm, 50.0 mm and 80.0 mm, respectively. These sets of images show that the modified method gives

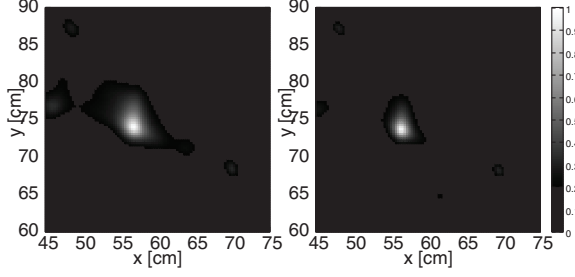


Fig. 5. Estimated image with the original frequency-domain DORT (left) and the modified frequency-domain DORT (right) for a target with radius of 30.0 mm.

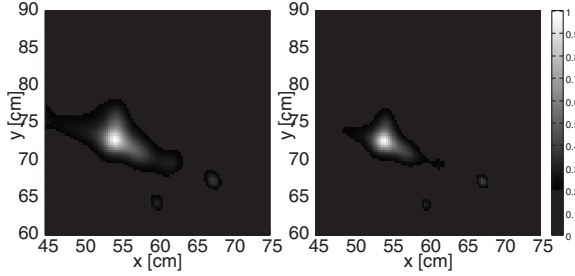


Fig. 6. Estimated image with the original frequency-domain DORT (left) and the modified frequency-domain DORT (right) for a target with radius of 50.0 mm.

sharper images than those from the conventional method. Here, we evaluate the quality of the images using the Muller and Buffington's (MB) sharpness metric [6]. The q -th order of this metric h_q is defined as

$$h_q = \frac{1}{M} \sum_{m=1}^M I_m^q, \quad (11)$$

where I_m is a vector with elements corresponding to pixel intensities normalized by the maximum pixel intensity of the image, and M is the number of pixels in the image. The exponent q determines the order of the statistics, meaning the sharpness of the image for $q > 2$ with higher-order statistics. Note that for this metric, small values of h_q signify sharper images. Here, we set $q = 4$ and evaluate image sharpness for the images given in Figs. 5, 6 and 7; the results are displayed in bar graph form in Fig. 8, from which it can be observed that the modified frequency-domain DORT achieves greater sharpness in all cases. Using our modified method, the image sharpness of the three targets in Figs. 5, 6 and 7 is improved by factors of 1.98, 1.78 and 1.34, respectively, over the conventional method.

VII. CONCLUSIONS

We proposed a UWB radar imaging method to improve image sharpness by introducing waveform compensation to the existing frequency-domain DORT. The original frequency-domain DORT method assumes propagation and scattering from a point-like target, decomposing a matrix calculated in

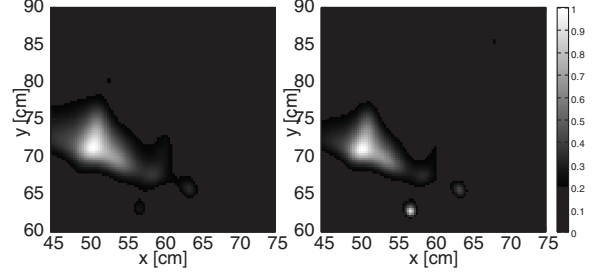


Fig. 7. Estimated image with the original frequency-domain DORT (left) and the modified frequency-domain DORT (right) for a target with radius of 80.0 mm.

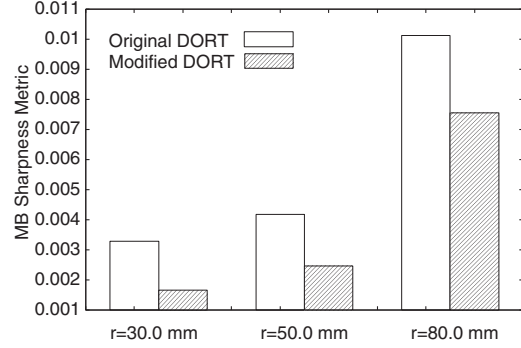


Fig. 8. Comparison of sharpness for the original and modified DORT images using the fourth-order Muller and Buffington's sharpness metric.

the frequency-domain using the singular value decomposition. The image is then calculated using a method based on the orthogonality between different vector subspaces. Treating the case of cylindrical metallic targets of different radii, this paper calculated the received signals using the FDTD method. The images obtained using data processed using the original frequency-domain DORT and the modified version were compared and quantified in terms of their image sharpness, thereby demonstrating the advantage of our modified method presented here.

REFERENCES

- [1] T. Sakamoto and T. Sato, "Time-reversal UWB imaging with a single antenna in multi-path environments," 3rd European Conference on Antennas and Propagation (EuCAP), pp. 2177–2181, 2009.
- [2] A. J. Devaney, "Time reversal imaging of obscured targets from multistatic data," IEEE Trans. Antennas and Propagat., vol. 53, no. 5, May 2005.
- [3] D. M. Fromm, C. F. Gaumont, J. F. Lingeitch, R. Menis, D. C. Calvo, G. F. Edelmann, E. Kim, "The effect of coherence and noise on the decomposition of the time reversal operator," Proc. MTS/IEEE OCEANS, pp. 1210–1215, 2005.
- [4] P. Simko, J. Saniie, "Computational time reversal ultrasonic array imaging of multipoint targets," Proc. IEEE ultrasonic symposium, pp. 1208–1212, 2007.
- [5] M. E. Yavuz and F. L. Teixeira, "Space-frequency ultrawideband time-reversal imaging," IEEE Trans. Geoscience and Remote Sensing, vol. 46, no. 4, Apr. 2008.
- [6] R. A. Muller and A. Buffington, "Real-time correction of atmospherically degraded telescope images through image sharpening," J. Optical Society of America, vol. 64, no. 9, pp. 1200–1210, 1974.